analytical chemistry

pubs.acs.org/ac Article

Thin-Layer Potentiometry for Creatinine Detection in Undiluted Human Urine Using Ion-Exchange Membranes as Barriers for Charged Interferences

Yujie Liu, Rocío Cánovas, Gastón A. Crespo, and María Cuartero*

Cite This: *Anal. Chem.* 2020, 92, 3315−3323 Read Online

ACCESS | Metrics & More | Article Recommendations | Supporting Information

ABSTRACT: Herein, thin-layer potentiometry combined with ion-exchange membranes as barriers for charged interferences is demonstrated for the analytical detection of creatinine (CRE) in undiluted human urine. Briefly, CRE diffuses through an anion-exchange membrane (AEM) from a sample contained in one fluidic compartment to a second reservoir, containing the enzyme CRE deiminase. There, CRE reacts with the enzyme, and the formation of ammonium is dynamically monitored by potentiometric ammonium-selective electrodes. This analytical concept is integrated into a lab-on-a-chip microfluidic cell that allows for a high sample throughput and the operation under stop-flow mode, which allows CRE to passively diffuse across the AEM. Conveniently, positively charged species (i.e., potassium, sodium, and ammonium, among others) are repelled by the AEM and never reach the ammonium-selective electrodes; thus, possible interference in the response can be avoided. As a result, the dynamic potential response of the electrodes is entirely ascribed to the stoichiometric formation of ammonium. The new CRE biosensor exhibits a Nernstian slope, within a linear range of response from 1 to 50 mM CRE concentration. As expected, the response time (15−60 min) primarily depends on the CRE diffusion across the AEM. CRE analysis in urine samples displayed excellent results, without requiring sample pretreatment (before the introduction of the sample in the microfluidic chip) and with high compatibility with development into a potential point-of-care clinical tool. In an attempt to decrease the analysis time, the presented analytical methodology for CRE detection is translated into an all-solid-state platform, in which the enzyme is immobilized on the surface of the ammonium-selective electrode and with the AEM on top. While more work is necessary in this direction, the CRE sensor appears to be promising for CRE analysis in both urine and blood.

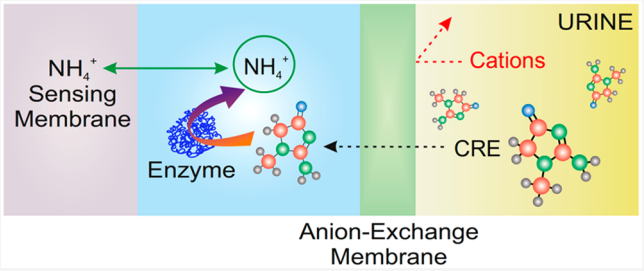

One of the most successful examples of a point-of-care (POC) device is the worldwide glucometer for glucose analysis in diabetic patients. Although there is no way to cure or prevent diabetes to date, medications that can be adjusted based on daily blood sugar monitoring have been shown to enhance treatment efficiency, alleviate the symptoms, and diminish the complications in patients' lives.[1,2] The management of diabetes has positively evolved over the years in response to the introduction of glucometers, which serves as an example for the development of POC devices capable of detecting other potential biomarkers for specific diseases. One of these molecules with a huge clinical interest is creatinine (CRE), which is connected to chronic kidney disease, muscular disorders, cardiovascular problems, and Parkinson disease.[3−5]

CRE is the second most analyzed biomolecule for clinical purposes, after glucose.[6] Indeed, CRE detection is included in routine blood and urinary tests to detect kidney malfunction. These analyses are performed in centralized clinical laboratories, after sample collection, and comprise the colorimetry-based Jaffé method.[7] Unfortunately, this method is not compatible with the POC detection of CRE, in addition to present severe chemical, pH, and temperature interferences.[8,9] Alternatives to the Jaffé method that have been proposed in the literature, primarily biosensors, have not achieved all the clinical requirements for CRE analysis yet. The main drawbacks are associated with the need for sample pretreatment (i.e., sample acidification and/or dilution) and strong interferences from other compounds present in the biological fluid being analyzed.[5,10,11] Thus, the Jaffé method is the only commercially available technique for clinical CRE analysis, to date.

In the direction of avoiding interferences in the analytical signal, a common trend in biosensor research has been the implementation of an external barrier that prevents other compounds from reaching the electrode surface. This concept

Received: November 18, 2019
Accepted: January 23, 2020
Published: January 23, 2020

https://dx.doi.org/10.1021/acs.analchem.9b05231
Anal. Chem. 2020, 92, 3315−3323

is based on the principle of restricting the diffusion of certain ions and (bio)molecules from the sample to the sensing core of the electrode.[12,13] Different materials can be used for this purpose, based on size exclusion and/or charge interactions. The most common example is the use of Nafion coatings that prevent anionic interfering species (such as ascorbate and urate) from reaching the electrode surface of lactate[13,14] and glucose[13,15] biosensors.

The polymeric structure of Nafion contains a hydrophobic ($-CF_2-CF_2-$) backbone and hydrophilic sulfonic acid groups ($-SO_3H$) that provide its well-known electron-withdrawing and cation-exchange properties. As a result, Nafion can repulse negatively charged species, with the additional advantage of remarkable (bio)fouling resistance during biological fluid measurements.[12,16] Although the suppression of anionic interferences by Nafion and other polymeric membranes with cation-exchange features has been widely demonstrated in the literature,[13,17−19] studies examining cationic interferences are lacking. A material that provides a similar barrier against cations would be useful during the preparation of biosensors that aim to detect any cation being formed during the enzymatic reaction in which the analyte is involved.

In the present article, we demonstrate thin-layer potentiometry for CRE detection in undiluted human urine by using an anion-exchange membrane (AEM) as a barrier against positively charged interferences. Using a new lab-on-a-chip microfluidic cell, the AEM is positioned between the sample and a solution containing CRE deiminase. Potentiometric ammonium-selective electrodes are in contact with the enzyme solution. Thus, all of the CRE that passes from the sample to the enzyme solution through the AEM is converted into ammonium ions (NH_4^+), whose activity is monitored by the potentiometric electrodes. Potential interference from any cation present in the sample is avoided due to the AEM, which impedes cations from reaching the electrodes. As a result, the generated NH_4^+ is selectively detected in real-time, allowing the CRE content in undiluted human urine to be analyzed. Combining the advantages associated with microfluidic lab-on-a-chip devices and those inherent to potentiometric readout, the developed analytical methodology for CRE detection presents a series of features that are clearly compatible with the development of a POC tool. Furthermore, the analytical performance of this method, in terms of response time and limit of detection, may be improved by translating the developed sensing strategy into an all-solid-state concept.

EXPERIMENTAL SECTION

Preparation of the Lab-on-a-Chip Microfluidic Cell for Creatinine Detection. All of the materials employed during the fabrication of the microfluidic cell are detailed in the Supporting Information. The design of the microfluidic cell for CRE detection is illustrated in Figure 1 (dimensions of 50 mm × 30 mm × 1 mm). Essentially, the microfluidic cell consists of several layers. (i) A plastic film of 50 mm × 30 mm × 0.1 mm in size, with two holes of 1.75 mm of diameter in the outer ends of the layer and separated by 35 mm (inlet and outlet of channel 2). In this first layer, four electrically conductive tape strips, sized 20 mm × 3 mm × 0.9 mm (labeled as 1 in the figure) were fixed to the plastic film. (ii) A plastic film with adhesive tape (sized 50 mm × 25 mm × 0.15 mm) with the same two holes in the outer ends as in (i) and four extra 2 mm diameter holes, which coincide with the ends of each carbon strip in (i). Of these four holes, three were filled with the

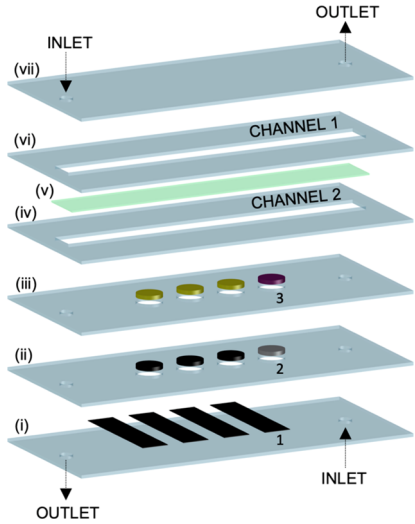

Figure 1. Illustration of the lab-on-a-chip microfluidic cell for CRE detection. (i) Plastic film where the conductive tape strips (1) are placed. (ii) Plastic film with four holes, where the carbon and silver pastes (2) are deposited for the preparation of the electrodes. (iii) Plastic film with the same four holes, where the membranes (3) are deposited. (iv) Fluidic channel for the enzyme solution. (v) AEM (FAPQ). (vi) Fluidic channel for the sample. (vii) Plastic layer to close the fluidics.

carbon-based paste and the last hole was filled with the silver/silver chloride (Ag/AgCl) paste (labeled as 2 in the figure). Afterward, the electrodes were cured at 100 °C in the oven for 10 min. (iii) A similar layer as described in (ii) was used to functionalize the electrodes (labeled as 3 in the figure). The three electrodes based on the carbon paste were subsequently modified by drop-casting of the multiwalled carbon nanotubes (MWCNTs) solution (10 × 0.5 μL) and allowing them to dry for 10 min. Then, the corresponding ion-selective membrane (ISM) was drop-casted on top of the MWCNT layer (10 × 1 μL). The final hole, containing the Ag/AgCl paste, was modified with the reference membrane (RM, 5 × 1 μL). Each layer was dried for 5 min before depositing the next drop. Finally, the ISMs and RM were left to dry, at room temperature, overnight. The next day, the RM was conditioned in 3 M KCl at least for 8 h using the drop method. In addition, just before use, all the electrodes were conditioned for at least 2 h by immersion in 100 mM NH_4Cl solution. (iv) A plastic film with adhesive tape in each side (50 mm × 25 mm × 0.2 mm), comprising the fluidic channel (40 mm long, with a cross-section of 3 mm × 0.2 mm and total internal volume of 24 μL, channel 2). The layers (iii) and (iv) were placed to align the electrodes with the fluidic channel. (v) The AEM, called FAPQ (45 mm × 13 mm × 0.075 mm), was placed to entirely cover the channel space. This membrane was hydrated in Milli-Q water before being implemented in the microfluidic cell. (vi) The same layer as described in (iv) was then placed, containing another microfluidic channel (channel 1). (vii) A plastic film (50 mm × 25 mm × 0.1 mm), with two holes for the inlet and outlet for this channel.

Other versions of the microfluidic cell were also prepared to perform control experiments (Figure S1a,b). The first version consisted of a cell containing a single fluidic channel comprising in turn three working electrodes and the reference electrode (Figure S1a). The second version contained an extra

https://dx.doi.org/10.1021/acs.analchem.9b05231
Anal. Chem. 2020, 92, 3315−3323

series of electrodes coupled to the second channel (Figure S1b).

RESULTS AND DISCUSSION

Figure 2 illustrates the working mechanism underlying the analytical methodology for CRE detection (i.e., the lab-on-a-chip CRE biosensor). Essentially, this method is based on a microfluidic cell (Figure 1), comprising two channels that are separated by the AEM: where one channel (channel 1) contains the sample and the other (channel 2) contains the CRE deiminase enzyme solution at physiological pH (phosphate buffer at pH 7.4, PB). Both solutions are confined to thin gaps (<0.2 mm, considering the channel thickness and a possible emplacement of the sensing membranes after the assembly of the chip). Three all-solid-state potentiometric ammonium-selective electrodes, together with the Ag/AgCl reference electrode, are implemented in the channel 2 containing the CRE deiminase solution. Notably, a number of three electrodes were selected to provide reproducibility for CRE analysis.

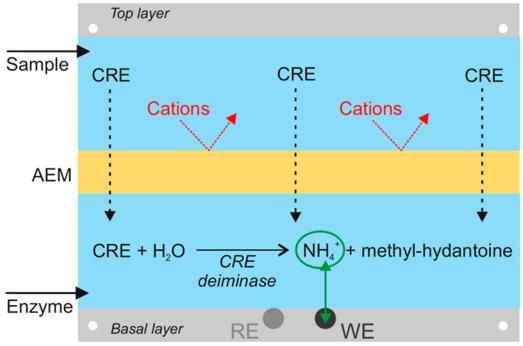

Figure 2. Illustration of the working mechanism underlying CRE detection in the microfluidic cell. CRE, creatinine; AEM, anion exchange membrane; CRE deiminase, creatinine deiminase (enzyme); WE, working electrode; RE, reference electrode.

First, the layer containing the ammonium-selective electrodes (n = 3) and the reference electrode (assembly containing layers (i–iii) in Figure 1) was analytically tested in batch mode (Figure S2 in Supporting Information). A Nernstian slope was observed for the three electrodes (57.01 ± 0.02 mV), within a wide linear range of response (from 10^{-6} to 10^{-1} NH_4^+ activity), a fast response time (15–30 s, within the linear range of response), a limit of detection of 10^{-7} NH_4^+ activity, and excellent between-electrode reproducibility (relative standard deviation RSD of 0.1% for slope magnitude), when the commercial Ag/AgCl reference electrode was used (Figure S2a,b). Advantageously, the analytical performances of the electrodes against the custom-made Ag/AgCl reference electrode were significantly similar to the measurements using the commercial one (Figure S2c).

The separate solution method was used to study the selectivity toward sodium and potassium ions, the two main interferences in nonactin-based membranes (see Figure S2d for the calibration graphs). The logarithmic selectivity coefficients were calculated to be $\log K_{NH_4,Na} = -2.9 \pm 0.1$ and $\log K_{NH_4,K} = -0.8 \pm 0.1$. As expected, a remarkable potassium interference was found, being ammonium detection only possible when potassium activity is between 1 and 2 orders of magnitude higher than ammonium activity.[20] Considering that the potassium concentration in urine is 20 mM on average, the indirect detection of CRE by measuring ammonium (after stoichiometric enzymatic conversion) would not be possible at the expected CRE levels, which are 3–20 mM in healthy subjects and <3 and >20 mM in potential clinical patients. Consequently, the suppression of potassium interference is convenient.

After characterizing the potentiometric electrodes in batch mode, we implemented the electrodes in a microfluidic cell containing only one microfluidic channel, according to the design shown in Figure S1a in the Supporting Information. This configuration, which is simpler than the lab-on-a-chip microfluidic cell for CRE detection (Figure 1), was preferred for these preliminary studies. Figure 3a depicts the dynamic response of increasing NH_4^+ activity in PB (pH 7.4) at both a constant flow of 30 μL min^{-1} and stop flow (indicated with pink arrows).

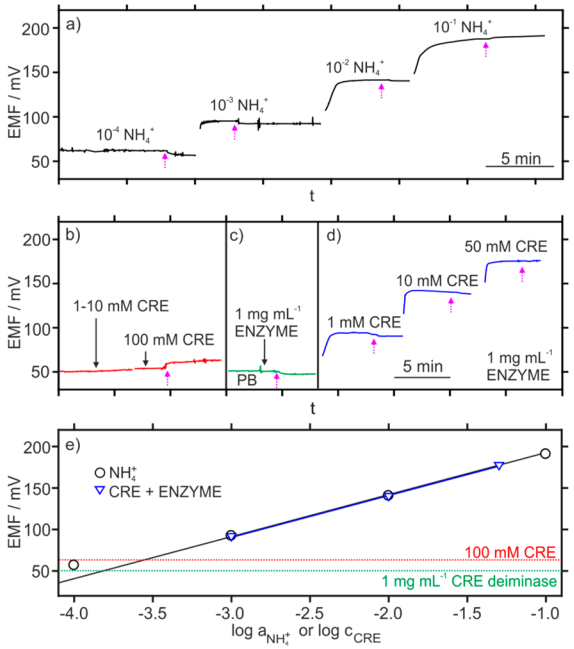

Figure 3. Potentiometric responses using the microfluidic cell based on a single channel (illustrated in Figure S1a). (a) Increasing ammonium activity. (b) Increasing concentrations of CRE. (c) CRE deiminase solution of 1 mg mL^{-1} concentration. (d) Increasing concentrations of CRE after being mixed with the enzyme solution. (e) Corresponding calibration graphs together with the response displayed for 100 mM CRE (red dotted line) and the CRE deiminase solution (green dotted line).

The corresponding calibration graph is shown in Figure 3e (black line and dots). The observed slope was the same as that observed in the beaker, and the linear range of response was displayed from $10^{-3.5}$ to 10^{-1} NH_4^+ activity; the response time was 70–160 s for activity changes within the linear range of response, and the limit of detection was $10^{-3.7}$ NH_4^+ activity. The linear range of response was narrower and the limit of detection higher than those observed in the batch mode because of the PB background (which contains Na^+ ions) used in the calibration graph. However, the PB background at pH 7.4 represents the optimal condition for the CRE deiminase enzymatic activity.[21]

Next, the response of the electrodes to increasing CRE concentrations (in the range of 1–100 mM) was also

https://dx.doi.org/10.1021/acs.analchem.9b05231
Anal. Chem. 2020, 92, 3315–3323

evaluated. As observed in Figure 3b, only a slight change in the potential signal was registered at 100 mM CRE concentration. However, the observed value was lower than that provided by $10^{-3.5}$ NH_4^+ activity (60 versus 75 mV). Because the linear range of response of the electrode was within $10^{-3.5}$ to 10^{-1} NH_4^+ activity, no significant interference was expected. Furthermore, any interference from the enzyme solution in the electrode response was also discarded for the same reason, based on the potential response of 1 mg mL^{-1} CRE deiminase in PB presented in Figure 3c (47 versus 75 mV).

It was also checked that ammonium detection after the interaction of CRE with the enzyme was possible by using the potentiometric ammonium-selective electrodes. Thus, CRE solutions at different concentrations were thoroughly mixed with 1 mg mL^{-1} of CRE deiminase in PB and then measured in the microfluidic cell. The observed dynamic response for the ammonium-selective electrode is displayed in Figure 3d. The enzyme concentration was selected to ensure that the reaction occurs stoichiometrically; therefore, 1 mol of CRE generates 1 mol of NH_4^+, instantaneously in PB medium.[22,23]

As expected, the higher the CRE concentration of the sample, the more NH_4^+ was formed in the reaction, and, consequently, the potential registered by the electrode increased. Moreover, the NH_4^+ activity, detected as a product of the CRE enzymatic reaction, perfectly corresponds with the initial calibration graph for NH_4^+ (see the black and blue lines in Figure 3e). This indicates that the reaction occurs stoichiometrically. In addition, the linear fitting found from 1 to 50 mM CRE concentration includes the expected CRE content in human urine (3−20 mM for healthy levels as well as <3 and >20 mM for harmful levels).[24,25]

When attempting CRE detection in human urine, many cationic species in the complex matrix of urine could influence the potentiometric response of the ammonium-selective electrode, especially the high levels of potassium and sodium ions as well as ammonium itself present in urine. The coupling of the AEM with the lab-on-a-chip microfluidic cell, as described in Figure 1, remarkably suppressed those interfering factors. Consequently, we analytically characterized the ability of the new lab-on-a-chip biosensor to determine CRE in undiluted human urine.

The ammonium-selective electrodes were first calibrated at increasing ammonium concentrations in the microfluidic cell (Figure 1). Figure 4a shows one of the obtained calibration graphs (a slope of 67.65 mV, a linear range of response from $10^{-3.5}$ to 10^{-1} NH_4^+ activity, a response time of 150−300 s, and a limit of detection of $10^{-3.7}$ NH_4^+ activity). In this experiment, the same NH_4^+ solution was placed in both channels of the microfluidic cell to avoid any activity gradient on both sides of the AEM. Importantly, the linear range of response was the same as that observed in previous experiments (see Figure 3). In principle, the use of the enzyme in PB (with Na^+) does not impede CRE detection in urine and the incorporation of the AEM will suppress much remarkable interference from K^+ (and other cations) present in the sample.

Subsequently, the CRE calibration was performed. For this purpose, the enzyme solution (1 mg mL^{-1} of CRE deiminase) was passed through channel 2, which contained the electrodes, and the CRE samples of the corresponding concentrations were passed through channel 1, simultaneously. After both channels were entirely filled (approximately 1 min), the flow was stopped to allow CRE to diffuse through the AEM into

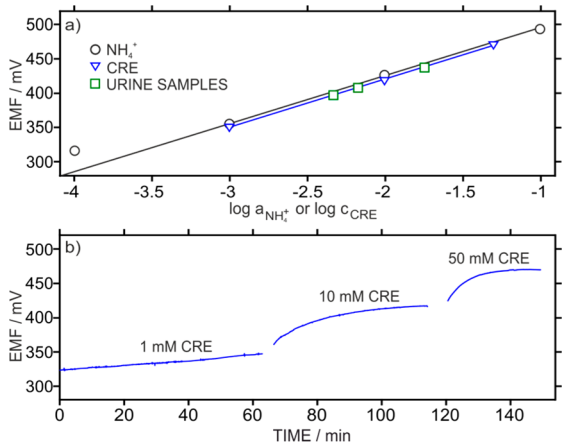

Figure 4. (a) Calibration graphs observed for ammonium and creatinine in the microfluidic cell illustrated in Figure 1. The potentials registered for the three urine samples are also shown. (b) Dynamic response of the ammonium-selective electrode at increasing concentration of creatinine, using the microfluidic cell illustrated in Figure 1.

channel 2, containing the enzyme solution. This diffusion occurs spontaneously, based on the concentration gradient established for CRE on both sides of the AEM. When CRE interacts with the enzyme, methyl-hydantoin and NH_4^+ are generated (see Figure 2). The generated NH_4^+ is continuously detected by the ammonium-selective electrodes.

Figure 4b presents the dynamic potential profile for increasing CRE concentrations. It is evident that longer response times are now displayed compared to the previous NH_4^+ calibration, because of the CRE diffusion across the AEM. The response time decreased for increasing CRE concentrations, requiring approximately 60, 30, and 15 min for 1, 10, and 50 mM CRE concentration, respectively. However, the steady-state potential reached for every CRE concentration corresponds with that provided for equivalent NH_4^+ activity, as shown in Figure 4a. This points out that the CRE is completely transformed into NH_4^+ upon diffusion to channel 2. Consequently, the CRE reaction acts as a sink for all the CRE arriving from the sample, such that an equal concentration gradient across the AEM only occurs at trace amounts of CRE. Indeed, this does not affect the electrode response.

Advantageously, the steady-state potential registered by the ammonium-selective electrode followed a linear relationship for CRE concentrations ranging from 1 to 50 mM (Figure 4a, blue marks), with a slope of 67.74 mV, and was reproducible for both increasing and decreasing CRE concentrations, therefore demonstrating appropriate reversibility (<1% of variation in the potential displayed by the lower and the higher CRE concentrations in the calibration graph). Importantly, although the linear range of response is suitable for CRE detection in human urine, the ability of the AEM to act as a barrier to prevent cationic species from reaching the electrode surface must be evaluated.

We first confirmed that the enzyme cannot diffuse into channel 1. If this occurs, CRE reaction with the enzyme will also take place in the sample, and therefore, the ammonium concentration detected by the electrodes in channel 2 will provide underestimation of the CRE content. Thus, one experiment was performed with the CRE solution in the channel comprising the ammonium-selective electrodes

https://dx.doi.org/10.1021/acs.analchem.9b05231
Anal. Chem. 2020, 92, 3315−3323

(channel 2) and the enzyme solution in the other channel (channel 1), i.e., the opposite position for the solutions than that used for the regular CRE detection. This experiment did not result in any potential change with increasing CRE concentrations (data not shown), demonstrating that the enzyme does not pass through the AEM. Although the enzyme is a neutral compound, which is not repelled by the AEM structure, it likely does not diffuse across the membrane due to size exclusion issues.

We then demonstrated that only anions diffused across the AEM. For this purpose, we developed a third version of the microfluidic cell, in which a second series of electrodes were implemented in channel 1 (see Figure S1b in the Supporting Information). In this microfluidic cell, all of the electrodes used were all-solid-state chloride selective electrodes,[26] to monitor chloride activity on both sides of the AEM when a concentration gradient has been established. Figure S3a depicts the dynamic concentration profiles observed for chloride ions when solutions of 200 mM KCl and 1 mM KCl concentration are placed in the channels at both sides of the AEM at stop flow conditions. The potential readouts for the electrodes were converted into chloride concentrations, using a previous calibration graph. As expected, the chloride concentrations in both channels evolved until the same constant value was reached, close to 100 mM chloride concentration.

For regular diffusion processes (depending on mass transport across permselective films), the total number of moles is equally divided on both sides, considering that there is no accumulation in the film (or membrane). In the developed microfluidic cell, both channels have the same volume; therefore, the same chloride concentration was reached at the steady-state, which took approximately 35 min. Chloride diffusion across the AEM began very quickly from the compartment containing 200 mM KCl (the green line in Figure S3a). The electrodes were not able to detect this initial amount but were able to detect the evolution of the chloride concentration as well as its final value. These results fully demonstrated the diffusion of anions through the AEM used in this study (specifically FAPQ). The same type of experiment was performed using a cell containing potassium-selective electrodes, and no diffusion of potassium ions was detected (i.e., the potassium-selective electrodes displayed a constant signal over time). This result is in accordance with the anionic potentiometric response of AEMs of different nature, including FAPQ, previously reported.[27,28]

Because neutral molecules in the sample are able to diffuse across the AEM, we also tested the response of the CRE biosensor to both urea and creatine (Figure S3b). After calibrating the electrodes using increasing NH_4^+ concentrations, individual urea and creatine solutions, at 200 mM and 0.27 mM concentration, respectively, were measured. These concentrations are reflective for the concentrations found in urine.[29,30] The responses for urea and creatine fell outside the linear range of response for the electrode, indicating that neither of these two compounds sufficiently reacted with the CRE deiminase (assuming that these compounds successfully diffuse across the AEM). Indeed, the potential values of the electrode for urea and creatine were close to that observed in the PB background. Conversely, the 1 mM CRE solution resulted in a potential signal similar to that observed for 1 mM NH_4^+ activity, as demonstrated in our previous experiments. The same trend was found when 1 mM solutions of KCl, NaCl, and NH_4Cl were measured. As a result, no interference is expected for the detection of CRE in undiluted human urine as a consequence of the matrix effect.

The reproducibility of the analytical performances for CRE detection as well as the lifetime were also evaluated. For this purpose, CRE calibration graphs were obtained in the following cases: (i) three subsequent calibration graphs for the same electrode, (ii) one calibration graph for the three electrodes in the same microfluidic cell, (iii) one calibration graph for different cells, and (iv) calibration graphs for the same electrode in consecutive days. In all the cases, we found an excellent reproducibility for the calibration parameters, with <5% of variation for the slope and intercept in the case of different microfluidic cells (see Table S1 in the Supporting Information). The lifetime of the cell once it was assembled (and the electrodes kept in the conditioning solution) was 5 days. From the fifth day, the response displayed a marked decreased, probably due to a fail in the reference membrane, because it cannot be reconditioned (or stored) at high KCl concentrations to preserve its constant potential. Another advantage of the sensors is that a very low drift was registered at medium-term in the presence of 10 mM NH_4Cl and 10 mM CRE (30 and 50 $\mu V\ h^{-1}$, respectively).

After characterizing the developed CRE biosensor, eight urine samples from different healthy volunteers together with two spiked samples were analyzed. These two later samples were additionally prepared to cover the detection of higher CRE levels in urine. CRE concentrations in undiluted urine samples were calculated by comparing of the potential readouts of each sample with the CRE calibration graph (see Figure 4a). In addition, the CRE contents in these samples were obtained using an existing commercial kit for CRE detection in biological fluids, which is based on the Jaffé method. Table 1 shows the results. In general, respectable correspondence between the two methods was observed as well as acceptable recoveries in the case of spiked samples, confirming the accuracy of the developed analytical methodology for the determination of CRE concentration in undiluted human urine. Furthermore, the new CRE biosensor allows for noninvasive urine analysis using just a few microliters of sample (24 μL), with no need for sample pretreatment (such as dilution and/or acidification). In addition, the linear range of response allows for the differentiation between healthy and harmful CRE levels in urine. The fabrication of the lab-on-a-

Table 1. Creatinine Analysis in Human Urine[a]

sample	colorimetric kit (mM)[b]	this work (mM)[c]	% diff[a]	% recovery
1	5.75 ± 0.26	6.05 ± 0.98	5.26	
2	4.03 ± 0.11	4.13 ± 0.78	2.58	
3	16.08 ± 0.73	18.12 ± 0.10	12.65	
4	4.04 ± 0.24	4.71 ± 1.21	16.58	
5	7.76 ± 0.44	8.31 ± 0.23	7.09	
6	3.98 ± 0.40	4.53 ± 0.77	13.82	
7	7.02 ± 0.14	8.02 ± 1.11	14.25	
8		4.25 ± 0.95		
8[d]		15.31 ± 1.20		107
8[e]		27.12 ± 1.37		111

[a]%Diff: difference between the creatinine contents found using the developed microfluidic cell and those found using the colorimetric kit. [b]Average of three measurements. [c]Average of three electrodes. [d]Sample number 8 plus 10 mM CRE. [e]Sample number 8 plus 20 mM CRE.

https://dx.doi.org/10.1021/acs.analchem.9b05231
Anal. Chem. 2020, 92, 3315−3323

chip microfluidic cell and the electrodes is cost-effective and compatible with a disposable concept, if necessary. The developed analytical strategy for urine analysis is presented in a lab-on-a-chip platform (dimensions of 50 mm × 30 mm × 1 mm) that would support the incorporation of a printed circuit board for wireless readout and automation, therefore providing total portability. In addition, the potentiometric readout of the electrodes is very easily interpreted.

The primary drawback of the developed technology may be the response time (15−60 min, depending on CRE concentration in the sample), which could be shortened when translating the sensing concept into an all-solid-state platform, as shown below, by controlling membrane thickness and nature. However, the discussed features make the developed strategy especially promising for CRE analysis in a clinical context compared with other approaches reported in the literature.

Several potentiometric electrodes have been reported over the years, but none have provided all of the requirements necessary for a CRE clinical test.[10,31−33] One common disadvantage associated with a majority of these sensors is the necessity of sample dilution and/or acidification. For example, the most recently published potentiometric CRE sensor is based on the detection of the creatininium cation, with the requirement that the biological fluid is buffered at pH 3.8 (i.e., at this pH, all the neutral CRE exists in the form of the creatininium cation, according to its pK_a). Moreover, the authors also claimed that the sample must be diluted, by a factor of 100 for urine and 10 for plasma, for the following two reasons: (i) to minimize biofouling and (ii) to fit in the corresponding linear range of response.[11,32] Despite the concept being very promising, the implementation of acidification and dilution pretreatments in a POC device would be rather complex.

This potentiometric electrode together with other strategies for CRE detection have been collected in a recent review.[5] One interesting point of the paper is the evaluation of some selected works according to its potential toward POC application for CRE analysis. This is currently the primary concern in CRE sensing, being the POC application absent in the majority of the (enzymatic) biosensors published from the 70s.[5] The following three approaches were highlighted. Dal Dosso et al. reported on a cartridge comprising a sampling zone and then a detection area that provides indirect colorimetric analysis of CRE after a cascade enzymatic reaction.[34] However, this approach is not compatible with urine analysis, and the preparation of the biosensor implies the use of several enzymes and other costly materials, which will impede the development of a cost-effective clinical tool.

Kumar et al. proposed a voltammetric sensor that follows the Fe^{3+}/Fe^{2+} redox conversion after the Fe^{3+} interaction with CRE.[35] This interaction was claimed to be CRE-concentration dependent. Although this approach is compatible with urine analysis and does not require any sample pretreatment, the main drawback is that the linear range of response only includes healthy CRE levels, and long-term stability, disposability, and interferences were not discussed. The authors recently reported on the use of the described technology in an impressive clinical study including patients with kidney dysfunction.[36]

Fu and co-workers demonstrated the implementation of the Jaffé reaction in a microfluidic paper-based analytical device (μPAD).[37,38] The μPAD allows for serum extraction from a few microliters of blood and then contains a reaction zone, with the analytical readout being performed in a portable detection box. This is an elegant concept that allows for a higher automation grade of the Jaffé method while reducing the need for sample manipulation. However, the disadvantages inherent to the Jaffé reaction are also presented by the μPAD, including strong sensitivity to specific interferences, temperature, and pH.[8,39]

To improve the response time, we have translated the developed concept for CRE analysis (ammonium detection + AEM as an interference barrier) into an all-solid-state format. Thus, the commercial glassy carbon (GC) electrode was modified with the following layers (in this order): MWCNTs, (as the ion-to-electron transducer), an ammonium-selective membrane (as the sensing element), CRE deiminase (as the biological element), and the AEM (as the physical barrier against cationic interferences). The reader is referred to the Supporting Information for a detailed description of the fabrication of the all-solid-state electrodes.

Figure 5a illustrates the working mechanism underlying the all-solid-state platform for CRE analysis. Essentially, when the electrode is immersed in the sample, CRE is expected to diffuse through the AEM reaching the enzyme that is entrapped at the interface with the ammonium-selective membrane. Then, CRE reacts with the enzyme and the generated NH_4^+ is detected by the ammonium-selective membrane. This new configuration may allow for two basic improvements. First, the thickness of the AEM can be controlled to allow the CRE deiminase to be well-entrapped and facilitate CRE diffusion across the membrane while continuing to repel cationic interferences. Importantly, reducing the AEM thickness is likely to reduce the analysis time compared with the microfluidic cell owing to a reduced AEM thickness. Second, the enzyme is physically immobilized at the interface between the ammonium-selective membrane and the AEM, avoiding the use of an enzyme solution in PB that worsens the limit of detection and linear range of the ammonium-selective electrode. While this is not an impediment for CRE detection in urine, the all-solid-state platform may reach CRE detection in blood, which is not accessible with the previous microfluidic cell.

Figure 5b−k shows the dynamic potential response of the all-solid-state CRE biosensors in different media, and Figure 5e presents the corresponding calibration graphs. The sensors were prepared by using AEM films that varied in terms of nature and thickness (number of layers or total deposited volume). First, we prepared the AEM using handmade solutions of the film materials FAPQ and FAA in *N*-methyl-2-pyrrolidone (NMP) and *n*-propanol, respectively. The concentrations used in the casted solutions (AEM material + organic solvent) were both 4 wt % and the materials were deposited on top of the enzyme layer.

Figure 5b,c depicts the dynamic potential at increasing CRE concentrations in two different media: PB and 0.01 M KCl solution. The CRE concentration at which a first potential change was registered varied depending on the AEM nature and the medium. Although both AEMs presented lower limits of detection and a linear range of response in KCl compared with PB (based on Na^+ ions), FAA displayed an enhanced response for CRE, and the response time appeared to be slightly faster (approximately 150 s versus >200 s). Considering the response of this electrode in 0.01 M KCl (the blue line in the right part of the figure, with a linear range

https://dx.doi.org/10.1021/acs.analchem.9b05231
Anal. Chem. 2020, 92, 3315−3323

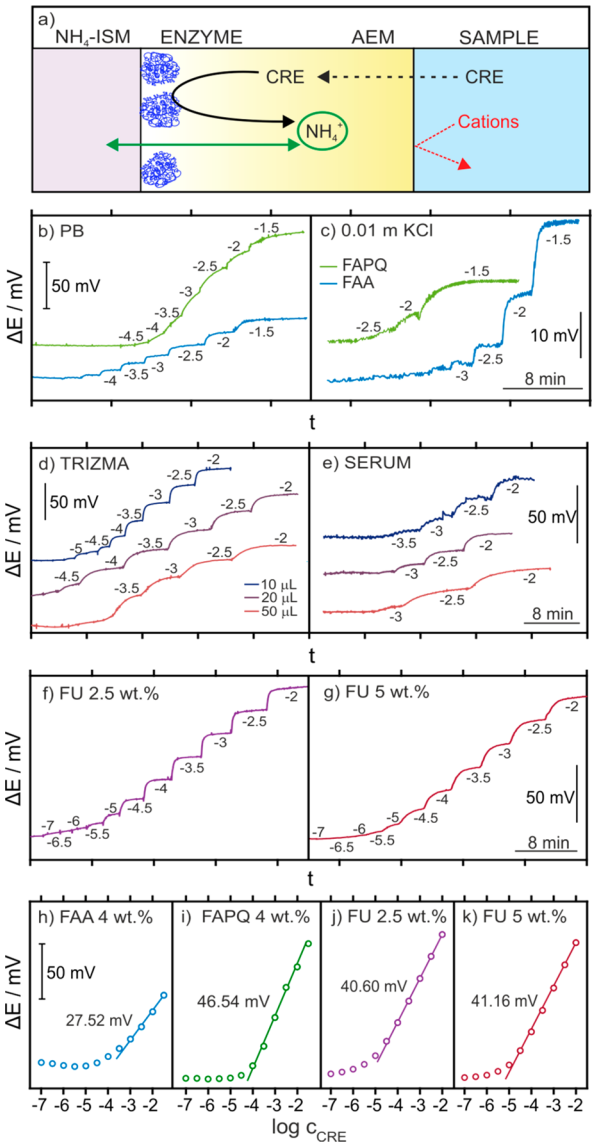

Figure 5. (a) Working mechanism underlying the all-solid-state creatinine biosensors. The responses of the electrodes prepared with FAPQ (NMP) and FAA (*n*-propanol) at 4 wt % (in the casted solution during its preparation) are displayed for increasing CRE concentrations in (b) PB and (c) 0.01 M KCl background. The responses of the electrodes prepared with different volumes of FAA, at 4 wt % (casted solution), in (d) trizma buffer and (e) artificial serum. The responses of the electrodes with (f) 2.5 wt % and (g) 5 wt % fumion (casted solution) in trizma buffer. Calibration graphs for (h) FAPQ (4 wt %) in PB, (i) FAA (4 wt %) in PB, (j) fumion (2.5 wt %) in trizma buffer, and (k) fumion (5 wt %) in trizma buffer. NH_4^+SM, ammonium-selective membrane; AEM, anion-exchange membrane; PB, phosphate buffer; FU, Fumion-based membranes. The numbers in the plots indicate the logarithmic concentrations of creatinine.

of response of 10^{-3}–$10^{-1.5}$ M), CRE detection in urine should be possible.

The CRE response of FAA-based electrodes was further evaluated using AEM films made from different deposited volumes (10, 20, and 50 μL) and, therefore, increasing thicknesses (Figure 5d,e). These electrodes were tested in trizma buffer at physiological pH and artificial serum to explore the possibility for blood analysis. The linear range of response for these electrodes started at a higher CRE concentration in artificial serum than in trizma, being from 10^{-3} to 10^{-2} CRE concentration in the best case. Therefore, these electrodes were not suitable for further CRE detection in human serum (the expected CRE levels in serum range from 40 to 150 μM).[38,40]

However, the response times were very similar in both media: ranging from 200 to 410 s in trizma buffer and from 210 to 450 s in artificial serum for increasing thickness. Thicker AEM resulted in longer response times for the sensors, likely because it takes more time for the CRE diffusion to reach the enzyme at the membrane–AEM interface. Notably, the observed response times were 10-fold faster than those in the microfluidic cell. However, these experiments did not clarify whether thicker membranes provide better repulsion of cationic species.

A commercial solution of fumion was also used to prepare the AEM layer in the biosensor, using two different dilutions at 2.5 and 5 wt % in NMP. Figure 5f,g presents the dynamic responses of these two electrodes in trizma buffer, with slopes of 40.60 and 41.16 mV, linear range of responses of $10^{-4.5}$–10^{-2} M, limits of detection of $10^{-5.2}$ M and 10^{-5} M, and response times of 80–100 s and 180–200 s, respectively. The primary difference between these two electrodes was the response time, which was faster for the membrane comprising the lower fumion content. This points out that the fumion concentration in the casted solution of the AEM is a factor that contributes to impeding the diffusion of CRE, likely because in a higher concentraton the croos-linked degree in the AEM is higher. As a result, both the polymer concentration in the AEM and the film thickness must be further optimized to reach a compromise between response time, interference suppression, and the linear range of response. Ideally, this latter should be from 10^{-5} to 10^{-2} M of CRE, which would encompass the average CRE levels in both human blood and urine.

In view of all these results, we can conclude that AEM-based electrodes containing fumion resulted in better calibration graphs for CRE at physiological pH (see Figure 5h–5k). Preliminary insights have shown that the limit of detection for fumion-based electrodes in buffer is 1.5 orders of magnitude lower than that observed for the lab-on-a-chip microfluidic cell ($10^{-5.1}$ M and $10^{-3.6}$ M, respectively). This fosters the potential for using this method to detect CRE in blood, in contrast to the restricted use of the microfluidic cell for urine analyses. Furthermore, faster response times can be achieved when using the all-solid-state platform due to faster CRE diffusion (200–400 s versus 15–60 min in the lab-on-a-chip microfluidic cell). Having demonstrated faster analysis times, we are now working to further optimize the fabrication process of this new generation of CRE biosensors, thus pursuing a sole electrode suitable for CRE analysis in undiluted human urine and blood/serum, with the aim of achieving a device suitable for POC clinical testing.

CONCLUSIONS

Creatinine (CRE) detection in undiluted human urine is possible using thin-layer potentiometry coupled to the anion-exchange membrane (AEM) FAPQ. The new lab-on-a-chip microfluidic cell allows the implementation of the AEM as a physical barrier against cationic interferences. The AEM is placed between two fluidic channels, one for the sample and the other containing the sensing element (CRE deiminase solution and a series of potentiometric ammonium-selective electrodes). This configuration provides selective CRE

https://dx.doi.org/10.1021/acs.analchem.9b05231
Anal. Chem. 2020, 92, 3315–3323

detection in urine within a 15−60 min time frame. The potentiometric ammonium-selective electrodes indirectly detected CRE through the formation of ammonium during its reaction with the enzyme CRE deiminase. The advantages of the developed analytical platform are as follows: small dimensions, compatibility with decentralized analysis and automation, noninvasive nature, the absence of biofouling, low sample volume requirement, reversibility, adaptable to disposability, and no need for sample pretreatments. The long response time may be overcome through the implementation of the concept for CRE sensing into an all-solid-state configuration. The preliminary results demonstrated the convenience of this new wave of sensors for the detection of CRE in urine and artificial serum. Despite further work being necessary in this direction, the developed technology appears to be suitable toward a sole biosensor for CRE detection in undiluted human urine and blood/serum, with further potential for point-of-care clinical testing.

■ ASSOCIATED CONTENT

Supporting Information

The Supporting Information is available free of charge at https://pubs.acs.org/doi/10.1021/acs.analchem.9b05231.

Experimental section; functioning of the two additional microfluidic cells prepared for control experiments; analytical performance of the ammonium-selective electrodes in batch mode and in the microfluidic cell; and chloride diffusion with a concentration gradient on both sides of the AEM (PDF)

■ AUTHOR INFORMATION

Corresponding Author

María Cuartero − *Department of Chemistry, School of Engineering Sciences in Chemistry, Biotechnology and Health, KTH Royal Institute of Technology 10044 Stockholm, Sweden;* orcid.org/0000-0002-3858-8466; Email: mariacb@kth.se

Authors

Yujie Liu − *Department of Chemistry, School of Engineering Sciences in Chemistry, Biotechnology and Health, KTH Royal Institute of Technology 10044 Stockholm, Sweden*

Rocío Cánovas − *Department of Chemistry, School of Engineering Sciences in Chemistry, Biotechnology and Health, KTH Royal Institute of Technology 10044 Stockholm, Sweden;* orcid.org/0000-0001-9552-535X

Gastón A. Crespo − *Department of Chemistry, School of Engineering Sciences in Chemistry, Biotechnology and Health, KTH Royal Institute of Technology 10044 Stockholm, Sweden;* orcid.org/0000-0002-1221-3906

Complete contact information is available at: https://pubs.acs.org/10.1021/acs.analchem.9b05231

Author Contributions

Y.L. and R.C have contributed equally to the research presented in this paper. Therefore, they share the first authorship.

Notes

The authors declare no competing financial interest.

■ ACKNOWLEDGMENTS

This project has received funding from the European Union's Horizon 2020 Research and Innovation Programme under the Marie Curie Sklodowska-Curie Grant Agreement 792824. The financial support of the Swedish Research Council (Grant VR-2019-04142) is also acknowledged. G.A.C. acknowledges the KTH Royal Institute of Technology (Grant K-2017-0371) and the Swedish Research Council (Project Grant VR-2017-4887). Y.L. gratefully thanks the China Scholarship Council for supporting her Ph.D. studies. R.C. thanks the financial support of the Alfonso Martin Escudero Foundation Fellowship. Special acknowledgement to Dr. Marc Parrilla for the initial discussion on the importance for creatinine sensing and to Alex Wiorek for the support in the preparation of the drawing of the microfluidic cell.

■ REFERENCES

(1) Yoo, E.-H.; Lee, S.-Y. *Sensors* **2010**, *10*, 4558−4576.
(2) Wang, J. *Electroanalysis* **2001**, *13*, 983−988.
(3) Killard, A. J.; Smyth, M. R. *Trends Biotechnol.* **2000**, *18*, 433−437.
(4) Diamond, B. J. *Temperature and pH Dependence of the Cyclization of Creatine: A Study Via Mass Spectrometry*. M.S. Thesis, Marshall University, Huntington, WV, 2005; 564.
(5) Cánovas, R.; Cuartero, M.; Crespo, G. A. *Biosens. Bioelectron.* **2019**, *130*, 110−124.
(6) Joffe, M.; Hsu, C.; Feldman, H. I.; Weir, M.; Landis, J. R.; Hamm, L. L. *Am. J. Nephrol.* **2010**, *31*, 426−434.
(7) Greenberg, N.; Roberts, W. L.; Bachmann, L. M.; Wright, E. C.; Dalton, R. N.; Zakowski, J. J.; Miller, W. G. *Clin. Chem.* **2012**, *58*, 391−401.
(8) Narayanan, S.; Appleton, H. D. *Clin. Chem.* **1980**, *26*, 1119−1126.
(9) He, Y.; Zhang, X.; Yu, H. *Microchim. Acta* **2015**, *182*, 2037−2043.
(10) Radomska, A.; Bodenszac, E.; Głąb, S.; Koncki, R. *Talanta* **2004**, *64*, 603−608.
(11) Guinovart, T.; Hernández-Alonso, D.; Adriaenssens, L.; Blondeau, P.; Rius, F. X.; Ballester, P.; Andrade, F. J. *Biosens. Bioelectron.* **2017**, *87*, 587−592.
(12) Emr, S. A.; Yacynych, A. M. *Electroanalysis* **1995**, *7*, 913−923.
(13) Hamdi, N.; Wang, J.; Monbouquette, H. G. *J. Electroanal. Chem.* **2005**, *581*, 258−264.
(14) Alam, F.; RoyChoudhury, S.; Jalal, A. H.; Umasankar, Y.; Forouzanfar, S.; Akter, N.; Bhansali, S.; Pala, N. *Biosens. Bioelectron.* **2018**, *117*, 818−829.
(15) Harrison, D. J.; Turner, R. F. B.; Baltes, H. P. *Anal. Chem.* **1988**, *60*, 2002−2007.
(16) Manowitz, P.; Stoecker, P. W.; Yacynych, A. M. *Biosens. Bioelectron.* **1995**, *10*, 359−370.
(17) Clark, L. C.; Duggan, C. A. *Diabetes Care* **1982**, *5* (3), 174−180.
(18) Fan, Z.; Harrison, J. *Anal. Chem.* **1992**, *64*, 1304−1311.
(19) Rosario, S. A.; Sig Cha, G.; Meyerhoff, M. E.; Trojanowicz, M. *Anal. Chem.* **1990**, *62*, 2418−2424.
(20) Guinovart, T.; Bandodkar, A. J.; Windmiller, J. R.; Andrade, F. J.; Wang, J. *Analyst* **2013**, *138*, 7031−7038.
(21) Shih, Y. T.; Huang, H. J. *Anal. Chim. Acta* **1999**, *392*, 143−150.
(22) Pundir, C. S.; Yadav, S.; Kumar, A. *TrAC, Trends Anal. Chem.* **2013**, *50*, 42−52.
(23) Mohabbati-Kalejahi, E.; Azimirad, V.; Bahrami, M.; Ganbari, A. *Talanta* **2012**, *97*, 1−8.
(24) Li, M.; Du, Y.; Zhao, F.; Zeng, J.; Mohan, C.; Shih, W.-C. *Biomed. Opt. Express* **2015**, *6*, 849.
(25) Ruedas-Rama, M. J.; Hall, E. A. H. *Anal. Chem.* **2010**, *82*, 9043−9049.
(26) Pankratova, N.; Cuartero, M.; Jowett, L. A.; Howe, E. N. W.; Gale, P. A.; Bakker, E.; Crespo, G. A. *Biosens. Bioelectron.* **2018**, *99*, 70−76.
(27) Grygolowicz-Pawlak, E.; Crespo, G. A.; Ghahraman Afshar, M.; Mistlberger, G.; Bakker, E. *Anal. Chem.* **2013**, *85*, 6208−6212.

(28) Cuartero, M.; Crespo, G. A. *J. Chem. Educ.* **2018**, *95*, 2172−2181.
(29) Clark, L. C.; Thompson, H. L. *Anal. Chem.* **1949**, *21*, 1218−1221.
(30) Chutipongtanate, S.; Thongboonkerd, V. *Anal. Biochem.* **2010**, *402*, 110−112.
(31) Magalhães, J. M. C. S.; Machado, A. A. S. C. *Analyst* **2002**, *127*, 1069−1075.
(32) Guinovart, T.; Hernández-Alonso, D.; Adriaenssens, L.; Blondeau, P.; Martínez-Belmonte, M.; Rius, F. X.; Andrade, F. J.; Ballester, P. *Angew. Chem., Int. Ed.* **2016**, *55*, 2435−2440.
(33) Meyerhoff, M.; Rechnitz, G. A. *Anal. Chim. Acta* **1976**, *85*, 277−285.
(34) Dal Dosso, F.; Decrop, D.; Pérez-Ruiz, E.; Daems, D.; Agten, H.; Al-Ghezi, O.; Bollen, O.; Breukers, J.; De Rop, F.; Katsafadou, M.; et al. *Anal. Chim. Acta* **2018**, *1000*, 191−198.
(35) Kumar, V.; Hebbar, S.; Kalam, R.; Panwar, S.; Prasad, S.; Srikanta, S. S.; Krishnaswamy, P. R.; Bhat, N. *IEEE Sens. J.* **2018**, *18*, 830−836.
(36) Kumar, V.; Hebbar, S.; Bhat, A.; Panwar, S.; Vaishnav, M.; Muniraj, K.; Nath, V.; Vijay, R. B.; Manjunath, S.; Thyagaraj, B.; et al. *Kidney Int. Reports* **2018**, *3*, 1110−1118.
(37) Fu, L. M.; Tseng, C. C.; Ju, W. J.; Yang, R. J. *Inventions* **2018**, *3*, 34.
(38) Tseng, C.; Yang, R.-J.; Ju, W.-J.; Fu, L.-M. *Chem. Eng. J.* **2018**, *348*, 117−124.
(39) Spierto, F. W.; MacNeil, M. L.; Burtis, C. A. *Clin. Biochem.* **1979**, *12*, 18−21.
(40) Randviir, E. P.; Banks, C. E. *Sens. Actuators, B* **2013**, *183*, 239−252.

https://dx.doi.org/10.1021/acs.analchem.9b05231
Anal. Chem. 2020, 92, 3315−3323